Complex structures in the calculated photoionization spectrum of CO in the 17–17.5 eV energy region

Bernard Leyh
Aspirant du Fonds National de la Recherche Scientifique, Belgium, Departement de Chimie Generale et de Chimie Physique, Institut de Chimie-B6, B.4000 Sart Tilman (Liege 1), Belgium

Gheorghe Raşeev
Laboratoire de Photophysique Moleculaire du C. N. R. S., Universite de Paris-Sud, F.91405 Orsay Cedex, France

(Received 22 February 1988; accepted 25 March 1988)

Complicated spectral features appear in the CO photoionization spectra between 17 and 17.5 eV photon energy. In order to interpret these processes, we refine in the present paper our previous model [B. Leyh and G. Raşeev, Phys. Rev. A **34**, 2920 (1986)] by introducing all the vibrational levels of the first three electronic states of CO^+. This more accurate treatment leads to two major results. The resonances at 17.1 and 17.3 eV are complex resonances resulting from the interaction between the Rydberg series converging to the $A\,^2\Pi$ and $B\,^2\Sigma^+$ ionic states: they can no more be assigned simply to Rydberg states converging to $CO^+B\,^2\Sigma^+$. The intermediate experimental feature at 17.2 eV, missing in our previous calculation, is now present in the theoretical spectrum. Mainly, this feature, which we have called composite resonance, is a broadened (by the experimental resolution) superposition of Rydberg states converging to the $A\,^2\Pi\ v^+ = 4$ state. In this paper, we present and analyze the vibrationally resolved cross sections and asymmetry parameter for the $X\,^2\Sigma^+ v^+ = 0$–3 and $A\,^2\Pi\ v^+ = 0$–4 states. These theoretical results are compared to recent experimental data by Leyh *et al.* [Chem. Phys. **115**, 243 (1987)] and by Hardis and co-workers (the preceeding paper).

I. INTRODUCTION

Much interest has been recently addressed to the understanding of the different mechanisms involved in molecular photoionization.[1–7] At moderate photon energy ($E < 20$ eV), the photoionization spectra and branching ratios usually display a rich resonant structure resulting from the autoionization of several Rydberg series converging to excited vibronic ionic states.[4,6,7]

Detailed experimental information—i.e., partial cross sections and photoelectron angular distributions with constantly increasing resolution—is nowadays available on a few diatomic, triatomic, and even polyatomic molecules.[1–4,8–11]

The simple model of one well-separated Rydberg series interacting with one continuum breaks down in many cases. A particularly interesting situation happens, e.g., when a discrete autoionized level (of valence or Rydberg character), called the "interloper," interacts with a dense series of Rydberg states converging to a higher threshold, both interacting with the continuum: this gives rise to a "complex resonance."[6,12,13]

An elaborate theory which takes into account all the required interactions is the two-step multichannel quantum defect theory (two-step MQDT)[14,15]: this theory has allowed the first *ab initio* calculations of the photoionization spectra including autoionization.[16,17] The vibrational motion has also been introduced, leading to vibrationally resolved cross sections and asymmetry parameters.[17] Two other approachs have been implemented for the study of resonant photoionization. First, a variational method based on the logarithmic derivative of the wave function developed by Le Rouzo and Raşeev and by Greene[18,19] and, recently, a Green's function approach in the framework of scattering theory by Sobolewski and Domcke.[20,21] Raşeev[19] introduced two electronic ionic states and calculated the cross sections at different internuclear distances whereas Sobolewski and Domcke[20,21] introduce in a model calculation two electronic ionic cores with their vibrational levels.

In a previous paper[17] (hereafter referred to as LR), we have presented theoretical vibrationally resolved partial cross sections and asymmetry parameters (β) for the photoionization of CO between 17 and 18.3 eV, i.e., in the region of the first members of the Rydberg series converging to $CO^+B\,^2\Sigma^+$ (R_B series). These calculations were compared with the experimental vibrationally resolved results of Leyh *et al.*[22] We concluded that paper by stating that, although the great majority of spectral features was reproduced by our calculations, discrepancies between theory and experiment occurred between 17 and 17.5 eV. In particular, an experimental structure at around 17.2 eV (72.1 nm)[22–24] did not appear in our theoretical spectra.

In those calculations, we introduced the vibrational motion for the $X\,^2\Sigma^+$ ionic core ($v^+ = 0$–3) and for the $B\,^2\Sigma^+$ core ($v^+ = 0,1$) but we considered the $A\ ^2\Pi$ ionic core as a single open channel without explicit consideration of the vibrational levels: this seemed justified by the fact that, in the spectral region studied, nearly all the observed resonances could be assigned to the Rydberg series converging to the $B\,^2\Sigma^+$ ionic state (LR). However, the $A\,^2\Pi\ v^+ = 3$, 4, and 5 thresholds are located at, respectively, 17.09 (72.5 nm), 17.28 (71.8 nm), and 17.45 eV (71.1 nm), i.e., in the critical region. We can therefore anticipate the appearance of complex resonances due to the presence of the Rydberg series converging to the above mentioned vibrational thresholds of

 0021-9606/88/140820-10$02.10

the $A\ ^2\Pi$ ionic state (we call them in the following R_A series).

In order to take into account these more complicated phenomena which had not been considered in our previous work (LR), we report here on new *ab initio* calculations with explicit introduction of the vibrational motion for the $CO^+ A\ ^2\Pi$ channels. This will allow us to reproduce properly the behavior at the different vibronic thresholds and the possible existence of complex resonances. A preliminary account of this work appeared in a view paper by Raşeev *et al.*[6]

The motivation for such a detailed theoretical work is the new experimental results obtained first of all by one of us[22] and very recently by Hardis and co-workers[25] (preceeding paper). In the former paper, vibrationally resolved cross sections for the X and A ionic states are presented both in the regions of the R_A and R_B series; a detailed analysis of the resonance assignments and decay in the 15–17 eV range is also presented.

II. THEORETICAL METHOD

The detailed description of the theoretical model has been given in our previous publication (LR). In the following we discuss briefly this model:

(i) It is based on the Born–Oppenheimer and Condon approximations. Furthermore, the electronic states are calculated in the diabatic representation. The wave function takes the following expression:

$$\Psi(r,R) = \Phi^{\rm el}(r,R)X^{\rm vibr}(R), \tag{1}$$

$$\Phi^{\rm el}(r,R) \cong \Phi^{\rm el}(r,R_c), \tag{2}$$

where $\Psi(r,R)$, $\Phi^{\rm el}(r,R)$, and $X^{\rm vibr}(R)$ are, respectively, the total, electronic, and nuclear wave functions. The second equation introduces the Condon approximation (where R_c is normally chosen as the R centroid or the equilibrium distance of the initial neutral state).

(ii) Each of the electronic wave functions $\Phi^{\rm el}(r,R_c)$ is calculated separately at the one configuration level of approximation. This is made possible by the use of the projection operator technique developed in LR. The interaction between these states is calculated by numerical integration over meaningful electronic coordinates.

(iii) The vibrational functions have been calculated using Morse potentials with parameters taken from Huber and Herzberg compilation.[26]

(iv) The collisional method used to obtain the photoionzation spectrum is a modified version (LR) of the two-step multichannel quantum defect theory (MQDT) introduced by Giusti-Suzor and Lefebvre-Brion[14] and discussed in detail by Giusti-Suzor and Jungen.[15] An essential point in working with collisional methods is the definition of channels which are identified by a set of quantum numbers. We use two types of channels: internal and asymptotic, which are appropriate, respectively, for the electron close to the nuclei and far from them. The quantum numbers $|i\nu^+\rangle$ refer to the electronic and vibrational states of the ion and are the same for the internal and asymptotic channels. The internal region channels of the continuum electron are eigenchannels labeled by β. They span the subspace of open and close channels in the usual spirit of the MQDT. The asymptotic channels of the continuum electron are identified by 1λ; they correspond only to the physically open channels. MQDT performs at each photon energy the transformation from the internal to the asymptotic channels.

(v) The assignment of the autoionizing states of Sec. IV are given in terms of eigenchannels β which have no pure quantum numbers 1λ. For simplicity we label them by the principal quantum number n (to fix the energy position), by the most important partial wave 1 and the molecular symmetry λ. To stress the mixing between the partial waves we put the 1 label between quotes.

(vi) The version of the two-step MQDT we have developed allows us to reduce the number of internal region channels considered in the calculation thus diminishing the computational effort. We eliminate from the MQDT calculation the eigenchannels with very small quantum defects as they do not contribute to the physics we are interested in. By this procedure, the number of asympotic channels remains the same as in the standard two step MQDT.

(vii) The calculation of the differential cross section and the angular distribution parameter β (not to be confused with the channel index defined above) is done using the Tully, Berry, and Dalton[27] formulation modified by Thiel.[28,29] To analyze our results we make use of the partioning scheme of Thiel[28,29] and of the resonance approach of Kabachnik and Sazhina.[30]

III. NUMERICAL CALCULATIONS

The computational difficulties linked with the present model arise from two origins:

(i) To reproduce properly the photoionization cross sections, particularly near the thresholds, it is necessary to introduce supplementary channels resulting from the existence of vibrational structure in all the ionic cores considered.

(ii) Just below the ionization thresholds, the great density of narrow high-n Rydberg states—the widths decrease as $(n-\mu)^{-3}$— requires a very dense energy grid. In the preceeding expression μ is the quantum defect.

We discuss now how we handle these difficulties, stressing the differences with the calculations presented in LR.

First of all, we have introduced in the present model the $\nu^+ = 0$–6 vibrational levels of the $CO^+ A\ ^2\Pi$ ionic state together with the vibrational levels $\nu^+ = 0$–3 of the $X\ ^2\Sigma^+$ state and $\nu^+ = 0,1$ of the $B\ ^2\Sigma^+$ state, already present in LR. The number of channels is now 164 (Σ and Π symmetry) instead of 65 in LR (the number of channels is given by the product of the number of vibronic ionic cores and of the number of β eigenchannels associated to the excited electron).

To highlight the role played by the different interactions in building up the final result, we have also performed model calculations (called in the following R_A model calculations) switching off the interaction between the R_B and R_A series and between the R_B series and the X continuum. These model calculations will permit us to distinguish between the different types of resonances present in the spectrum.

In the 17–17.5 eV region (72.9–70.8 nm), the *ab initio* energies of the R_A ($n \geqslant 10$) are much more reliable than the R_b ($n = 3$) ones. This results mainly from the fact that high-n energies are much less sensitive to the exact values of the quantum defeats μ than low-n ones. In order to have a similar level of accuracy for the two kinds of series, we have fitted the R_B quantum defects to the experimental values.

The second difficulty was linked to the energy mesh. We have used a very dense energy grid with a variable step in order to define at best each of the numerous resonances. More precisely, we describe each resonance by five points, located, respectively, at the resonance maximum (E_r) and at energies $E_r \pm 0.7\Gamma$ and $E_r \pm 1.5\Gamma$, where Γ is the width of the resonance. The use of such a symmetric procedure is justified by the high values of the Fano's q parameter (i.e., Lorentzian shape of the resonances) for the R_A $'d'\delta$ and $'s+d'$ σ series which dominate the photoionization spectra.[22]

For a few resonances, we have compared the results obtained by this procedure with those obtained by the usual one with a very small constant energy step ($0.026\,\mathrm{cm}^{-1}$): we have in this way verified that there is no shift of the resonance energies—this results from our hypothesis of energy-independent couplings— and that the intensities are well reproduced by the variable step procedure. This procedure is thus absolutely satisfactory for the angular integrated cross sections but is less justified for the differential cross sections and β curves. The shape of the resonances in the β curves is different from that in the cross sections and there is in many cases a small shift in the position of the resonance. We shall discuss this point further below.

IV. RESULTS AND DISCUSSION

A. Cross sections: Complex and composite resonances

The theoretical cross sections obtained within this framework are displayed in Fig. 1 for the $X\,^2\Sigma^+ v^+ = 0$–3 ionic states and in Fig. 2 for the $A\,^2\Pi$ $v^+ = 0$–4 ion states. The spectral region is the one described in the introduction (17–17.5 eV): it includes the energy around 17.2 eV of the experimental resonance which remained unexplained in our previous paper (LR).

As expected, we observe a very dense series of narrow resonances in all the energy range studied. These resonances are the high-n members ($n \geqslant 10$) of the Rydberg series converging to the $CO^+A\,^2\Pi^+$ $v^+ = 3$, 4, and 5 thresholds. This defines three groups of resonances located around, respectively, 16.95, 17.2 and 17.35 eV. The first group,—i.e., converging to $CO^+A\,^2\Pi^+$ $v^+ = 3$—is quasidegenerate with the $R_B 3'p'\pi\nu_R = 0$ state: the interactions between this R_B state and the R_A series together with their respective couplings to the different continua give rise to a complex resonance in the sense defined by Giusti-Suzor and Lefebvre-Brion.[12] Another complex resonance arise at about 17.35 eV, where R_B $3'p'\pi\nu_R = 1$ and $R_B 3'\,p'\,\sigma\,\nu_R = 0$ interact with the R_A series.

Contrary to these two situations, the $R_A \nu_R = 4$ series (around 17.2 eV) can be considered as not influenced by the Rydberg stastes converging to $CO^+B\,^2\Sigma^+$: to distinguish this case from the complex resonances, we shall call this type of macroresonance a "composite resonance." As explained in Sec. IV B this name can be justified in relation with the convoluted spectrum. To confirm the minor role played by the R_B series in this case of this resonance we have performed R_A model calculations (see Sec. III). We obtain very regular Rydberg series converging to $A\,^2\Pi$ $v^+ = 3$, $v^+ = 4$, and $v = 5$ thresholds with intensity proportional to the corresponding Franck–Condon factors. The intensity is five times higher than in the case of the calculation presented in Fig. 1 owing to the large dipole transition moment to the A state and the weak interaction with the X continuum. No series disappears or is weakened. Our results confirm therefore in great part the interpretation of Ogawa and Ogawa[24] who assigned the observed lines between 17.15 and 17.25 eV

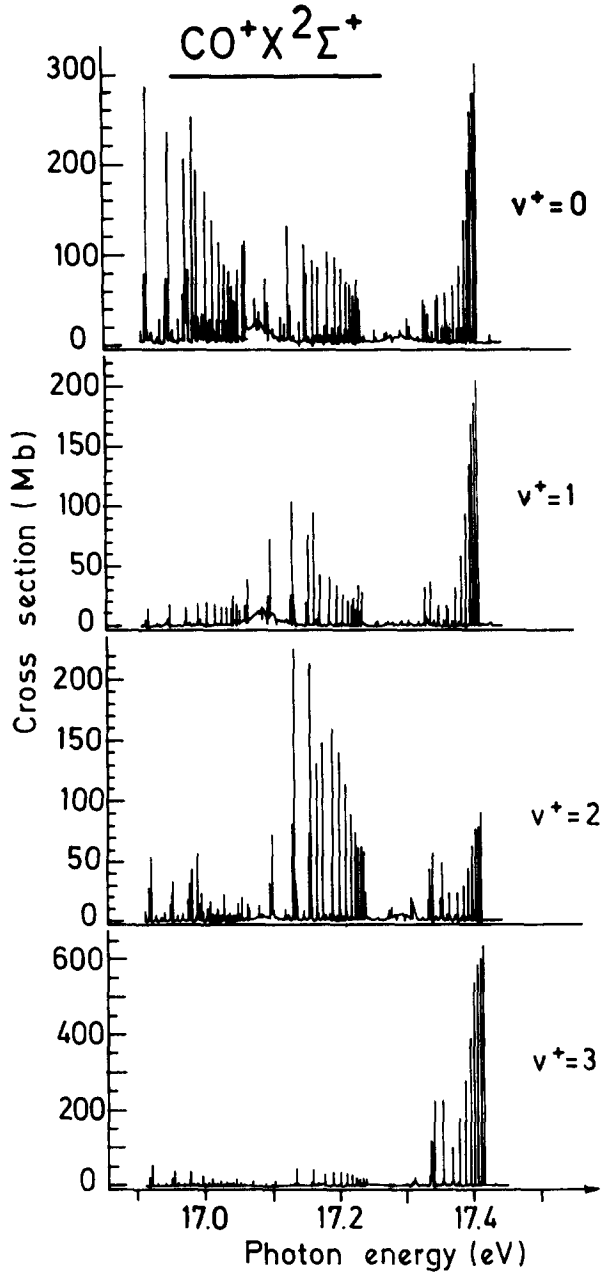

FIG. 1. Theoretical vibrationally resolved cross sections for the production of $CO^+X\,^2\Sigma^+v^+$.

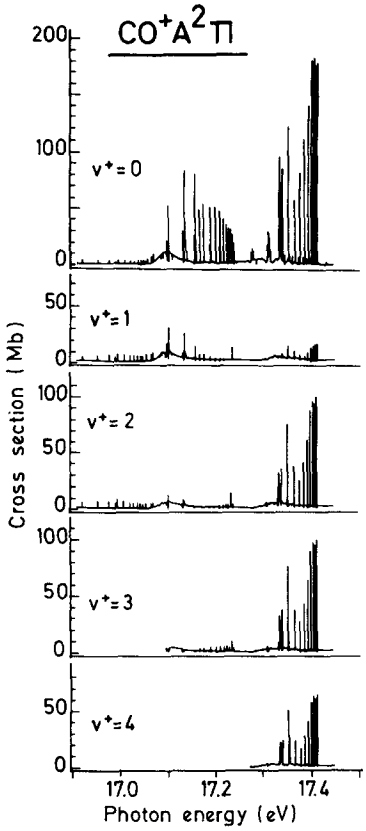

FIG. 2. Theoretical vibrationally resolved cross sections for the production of $CO^+A\ ^2\Pi\ v^+$.

to the $n = 9$–11 members of the $R_A \nu_R = 4$ series and to the $n = 7$ and $n = 8$ members of the $R_A \nu_R = 5$ series. We emphasize, however, that the situation is actually much more complicated than guessed by these authors, owing to the presence of a great number of Rydberg states in this region ($n \geqslant 10$)—and not only of five members— and also to the existence of three leading series (see below).

The comparison of Figs. 1 and 2 shows that the decay of the R_A states is more efficient in populating the X state than the A state. In fact, this selectivity in somewhat artificial in that it is a consequence of the use of the Condon approximation throughout this work (see Sec. II). This approximation is indeed equivalent to neglecting the pure vibrational autoionization.[6] In order words, at our level of approximation, the vibrational levels of the R_A states do not interact directly with the ionization continua corresponding to the different vibrational levels of the $A\ ^2\Pi$ ionic state. This interaction occurs however indirectly, and to a much weaker extent, via the A–X and B–A couplings: this leads to the observed spectral peaks. The R_A model calculations (see Sec. III) confirm the interpretation given above. We obtain weakened resonances (by a factor of 5) owing to smaller number of coupling path available. The comparison with the experimental results (see Fig. 4) will demonstrate that the Condon approximation is not valid for the $A\ ^2\Pi$ cross sections: it remains however satisfactory for the $X\ ^2\Sigma^+$ cross sections. Recent results by Delaval and Raşeev confirm this statement.[31]

A detailed assignment of the resonances appearing in Figs. 1 and 2 reveals that three series dominate the spectrum. These series are: $A\ ^2\Pi'(n+1)s + nd'\sigma$, $A\ ^2\Pi\ n'd'\delta$ which have high intensity and small width and $A\ ^2\Pi\ n'd'\pi$ which has relatively large width. The same is observed at lower energy for the first members ($n = 3$–6) of the R_A series.[22] As stated in Ref. 22, this behavior results from the quasihomonuclear nature of the 1π orbital from which the electron is excited: the most intense transitions are thus to Rydberg orbitals of *gerade* dominant character. These R_A resonances are characterized by high q parameters: as an example, for the $n'd'\delta\nu_R = 4$ series, one calculates a q value of 37.3; for the $'(n+1)s + nd'\sigma$ series, the corresponding figure is 138.8; for $'d'\pi$ series we obtain 13.9. These resonances display therefore a Lorentzian shape. The high q values result from the strong dipolar transition moment from the ground neutral state to the considered R_A states, and from the very weak autoionization widths (see Ref. 22). This situation thus leads to narrow spectral features with large cross sections at resonance. In the case of $n'd'\pi$ series this situation is attenuated owing to the smaller q parameter and to the larger width.

B. Convoluted cross sections: Comparison with experiment

In order to compare these theoretical results with the available experimental data, it is necessary to convolute them with an appropriate apparatus function. In Figs. 3 and 4, we present the convoluted cross sections for the different vibrational levels of the $X\ ^2\Sigma^+$ and $A\ ^2\Pi$ ionic states: these spectra are broadened to an experimental resolution of 0.05 eV and are compared with the results of Leyh *et al.*[22] The comparison (Fig. 5) between theoretical and experimental branching ratios is performed, only for the X state, using the results of Hardis *et al.*[25]: the resolution here is 0.017 eV.

The first observation one makes when looking at Figs. 3, 4, and 5 is that the calculated absolute cross sections are too high for the $X\ ^2\Sigma^+$ state but not for the $A\ ^2\Pi$ state. This results probably partially from an overestimation of the *ab initio* electronic discrete–discrete transition moments. On the other hand, we have pointed out that the Condon approximation leads to a selectivity in favor of the X state.

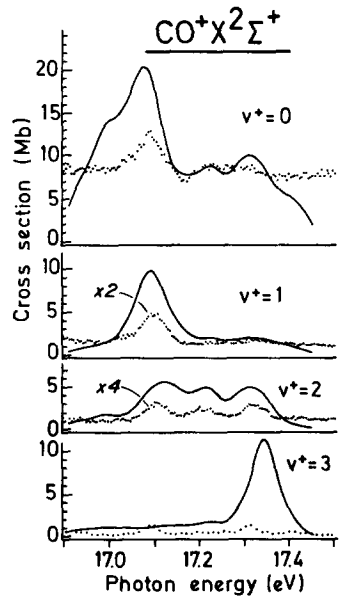

FIG. 3. Vibrationally resolved cross sections of the $X\ ^2\Sigma^+ v^+$ state. Solid line: theoretical results broadened to a resolution of 0.05 eV (0.2 nm). Dotted line: experimental results of Leyh *et al.* (Ref. 22).

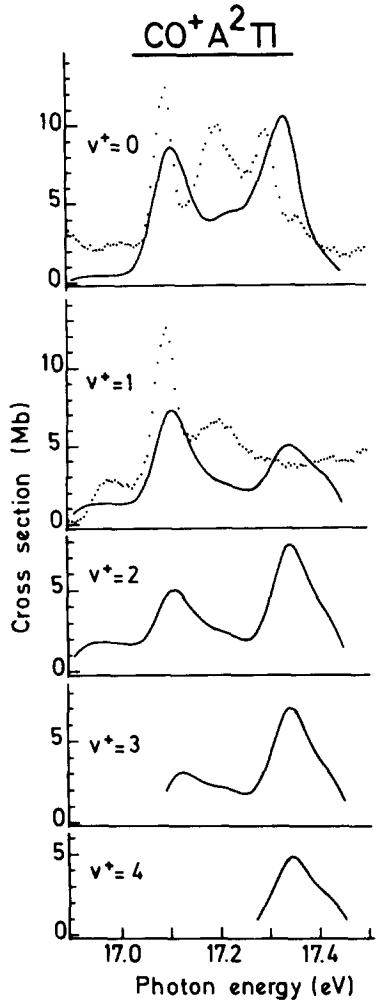

FIG. 4. Vibrationally resolved cross sections of the $A\ ^2\Pi$ state. Solid line: theoretical results broadened to a resolution of 0.005 eV (0.2 nm). Dotted line: experimental results of Leyh *et al.* (Ref. 22).

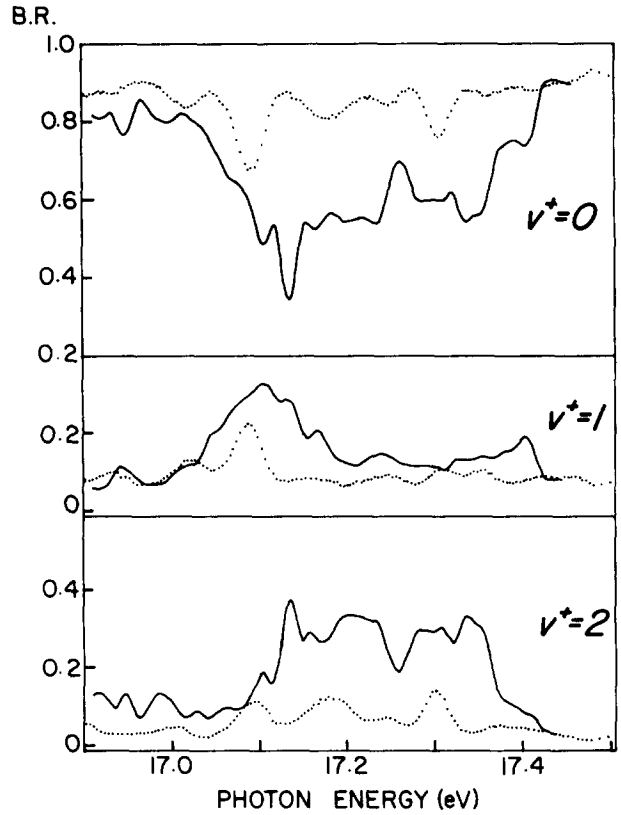

FIG. 5. Branching ratios of the $v^+ = 0$–2 vibrational levels of the $X\ ^2\Sigma^+$ state. To be comparable with the experiment the theoretical branching ratios (BR) are defined as $\sigma_{v^+}/(\sigma_{v^+=0} + \sigma_{v^+=1} + \sigma_{v^+=2})$. Solid line: theoretical results broadened to a resolution of 0.017 eV (0.065 nm). Dotted line: experimental results of Hardis *et al.* (Ref. 25).

Calculations beyond this approximation (i.e., introducing also the "pure" vibrational autoionization) should lead to a much fairer sharing between the A and X continua.

In contrast to this, the relative cross sections and the corresponding branching ratios are in much better agreement with the experimental results in particular for the X channels. This is not so surprising since the effects of overestimating the electronic transition moments will be the same in all the vibrational channels, at least within the Condon approximation.

Three features appear in the convoluted vibrationally resolved cross sections of the $X\ ^2\Sigma^+$ ionic state: as they result from the experimental broadening of a great number of narrow peaks, they can be called macroresonances. According to our discussion of the preceding subsection about the nonconvoluted results, the macroresonances at 17.1 and 17.3 eV are complex resonances. This means that they can no more be assigned simply as R_B resonances as was made in LR. The complex resonance mechanism is also confirmed by R_A model calculations (see Sec. III) which show features at 17.1 and 17.3 eV, the first being slightly shifted with respect to $R_B 3'p'\pi\nu_R = 0$ resonance (shoulder in Fig. 3) and the last being relatively weak. The enhancement by the R_B series for this last resonance seems relatively important. In these complex resonances, the interlopers are the R_B states which carry the oscillator strength and the R_A series are host series.

The intermediate macroresonances at about 17.2 eV results mainly from the $R_A \nu_R = 4$ series which are broadened to the experimental resolution (of width 0.017 eV) following the convolution procedure. As the experimental width is much larger than the average of the theoretical widths of the R_A series the result is an unique macroresonance which we call composite resonance. Of course the total area of the profile of the resonance is conserved by the convolution procedure. The appearance of this macroresonance is mainly due to the presence of the $3'd'\pi$ series which has relatively large widths (see also Ref. 22) and to the shift of the different series with respect to each other. Their weak interactions with the R_B series are confirmed by the R_A model calculations which after convolution show a feature similar to the one at 17.2 eV in Fig. 3. Therefore, in first approximation, this resonance is not a complex resonance since it can qualitatively been described by R_A model calculations. The composite resonance will display a behavior characteristic of the $v = 4$ vibrational wave function. This is illustrated by the variation of its intensity as a function of the vibrational level v^+ of the $X\ ^2\Sigma^+$ state. One sees (Figs. 3 and 5) that the decay of this macroesonance populates only the vibrational levels characterized by an even value of v^+. This behavior can be understood in the framework of the Condon approximation. The vibrational branching ratios for this autoionization process are given by the following Franck–Condon factors: $|\langle CO R_A \nu_R = 4 | CO^+ X\ ^2\Sigma^+ v^+ \rangle|^2$. The value of this

factor as a function of v^+ are: 0.1600 ($v^+ = 0$), 0.0058 ($v^+ = 1$), 0.0962 ($v^+ = 2$), and 0.0006 ($v^+ = 3$), thus explaining the observed experimental behavior.

Concerning the $A\ ^2\Pi\ v^+ = 0$–4 cross sections (Fig. 4), one notices that the experimentally observed composite resonance at 17.2 eV is not reproduced by the theoretical calculations. The calculations using the R_A model (see Sec. III) show no structure after convolution thus confirming the calculation with the complete model (Fig. 4). Furthermore, the experimental results show that this resonance contributes to populate the $A\ ^2\Pi\ v^+ = 0$ and 1 levels[22]: this corresponds to Δv values of -4 and -3, respectively, thus violating the Berry's propensity rule $\Delta v = -1$ for pure vibrational autoionization.[32] These results show therefore that neither the pure vibrational autoionization nor the electronic autoionization within the Condon approximation are appropriate to explain the decay of the composite resonance in the $A\ ^2\Pi\ v^+$ channels: a complete treatment taking into account all the X, A, and B channels and the variation with R of the associated electronic quantities (transition moments and interchannel couplings) is indispensable. We must mention that the breakdown of the $\Delta v = -1$ rule have also been observed in CO in another energy range by Ito *et al.*[33] Other examples include H_2,[34,35] NO,[15,36] and PF_3.[37]

C. Angular distribution of the electrons

In our preceding work (LR), we have calculated the angular distribution of the electrons and compared the results with the existing experimental data of Ederer *et al.*[38] covering only the energy region of the $R_B 3'p'\pi v_R = 0$ resonance. For each resonance in the angular integrated cross sections, we obtained a minimum in the angular asymmetry parameter β, in disagreement with the experiment. Here, the new experimental results of Hardis *et al.*[25] are compared with our new calculations.

The expression of the differential cross section is apparently very simple,

$$\frac{d\sigma}{d\Omega} = \sigma[1 + c\beta P_2(\cos\theta)], \tag{3}$$

where σ is the angular integrated cross section, c is a coefficient defined by the light polarization and by the geometry of the experiment, β is the asymmetry parameter, and $P_2(\cos\theta)$ is the second order Legendre polynomial. The asymmetry parameter β is written as a sum of products of the moduli of two complex transition moments times the cosine of their phase difference. Therefore, it contains complicated interference terms which are not present in the total cross section.

One of the possible analyses of β consists in considering the contributions to it of the different asymptotic or molecular channels. This is known as Thiel's partitioning scheme[28,29] and was applied in our previous paper (LR). Using this scheme, it is expected that one or at least very few contributions are predominant thus giving an insight in the mechanism of photoionization. The analysis presented in LR showed that there are many different contributions in the case of the $X\ ^2\Sigma^+$ state but only two in the case of the $A\ ^2\Pi$ state. This analysis is still valid here.

There also exists a global approach to study the variation of β across a resonance, developed by Kabachnik and Sazhina[30] and based on Fano's configuration approach.[39] In this approach, the complex transition moment (defined by its modulus and phase) is split into a resonant and a nonresonant part. An energy dependence of the transition moment near the resonance, similar to the well-known one for the angular integrated cross section,[39] emerges from this theory. From these transition moments Kabatchnik and Sazhina[30] obtain the following expression of the asymmetry parameter as a function of the reduced energy ϵ defined by Fano[39]:

$$\beta = (-2/\sigma)(X\epsilon^2 + Y\epsilon + Z)/(1 + \epsilon^2), \tag{4}$$

where σ has its own energy dependence and X, Y, and Z are written in terms of products of transition moments multiplied by a sine or cosine of the phase difference. The terms with nonzero phase difference are the interference terms. To highlight the contributions of these interference terms, we suggest to analyze our results in terms of $\sigma\beta$ instead of β: indeed, it has a simpler energy dependence than β and it corresponds to the maximum of the angular dependent term in the differential cross section [Eq. (3)].

The unconvoluted β curves corresponding to the $v^+ = 0$–3 levels of the X ionic state (Fig. 6) show an extremely oscillatory structure varying from -0.2 to 1.7. In the case of the $A\ v^+ = 0$–4 states (Fig. 7), the variation of β extends from -0.5 to 0.7. These variations are to be compared to the much smaller ones obtained in our previous work (LR). For the X state, this can easily been understood since the R_A series can now autoionize in the X continua: this lowers the minimum of β whereas the rise in its maximum value appears as a consequence of interference effects between the X and A channels. The β for the $A\ ^2\Pi\ v^+$ ionic states can only be compared with the existing electronic β calculations of LR. There is a rise in the minimum and maximum values which should originate in the greater number of continua an in the borrowing of the X state β character by the A state.

The analysis of the resonances appearing in the $X\ ^2\Sigma^+$ cross sections, in the framework of Thiel's partitioning scheme,[28,29] shows that there is now an important contribution from the β_{sd} and β_{dd} terms near the R_A autoionizing states.

In Sec. III, we have discussed our choice of the energy mesh in the context of the integrated cross section calculations. This choice is less justified in the case of the β as the form of the resonance is closer to the derivative of a Lorentzian function and furthermore, the resonance position can be slightly shifted with respect to the maximum observed in the integrated cross section.

We have convoluted the β curves at the experimental resolution of 0.017 eV (Figs. 8 and 9) obtained by Hardis and co-workers.[25] Comparison between experiment and theory shows mainly the same discrepancy as between the early results of Ederer *et al.*[38] and the theoretical model of LR. The new experimental data cover a much broader energy range and no shift in their relative energy position can bring experimental and theoretical curves in a better agreement.

As discussed above, we can also analyze the results in terms of $\sigma\beta$ which highlights the behavior of the interference

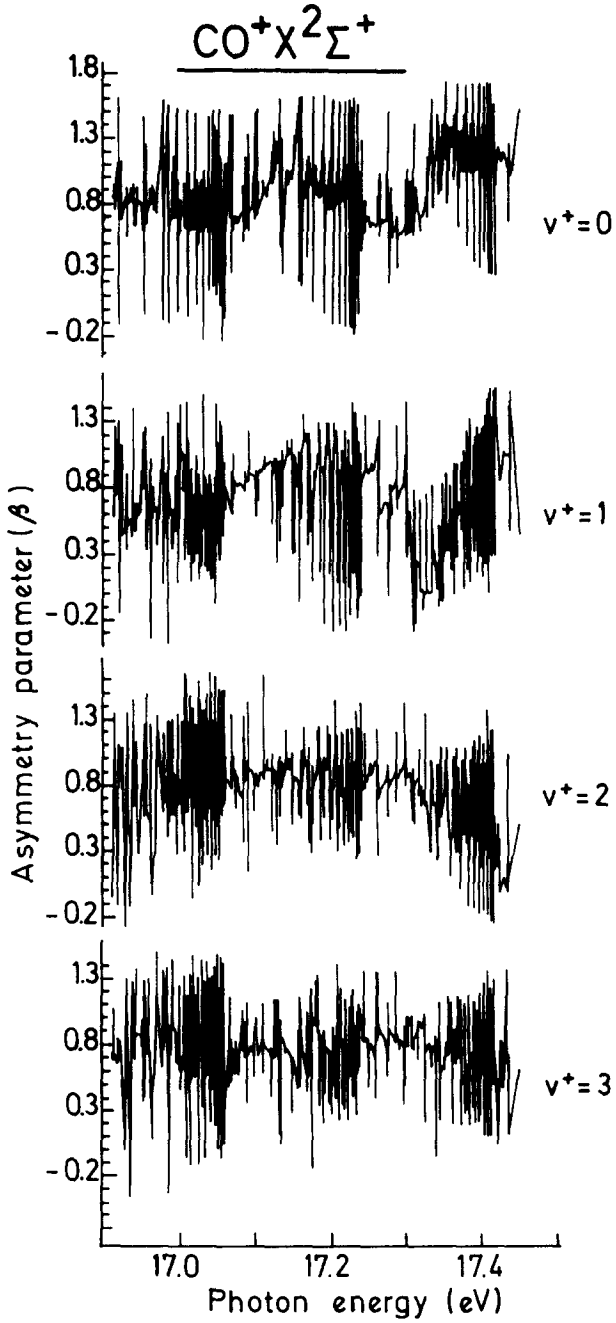

FIG. 6. Variation with photon energy of the $X\,^2\Sigma^+$ vibrationally resolved asymmetry parameter β.

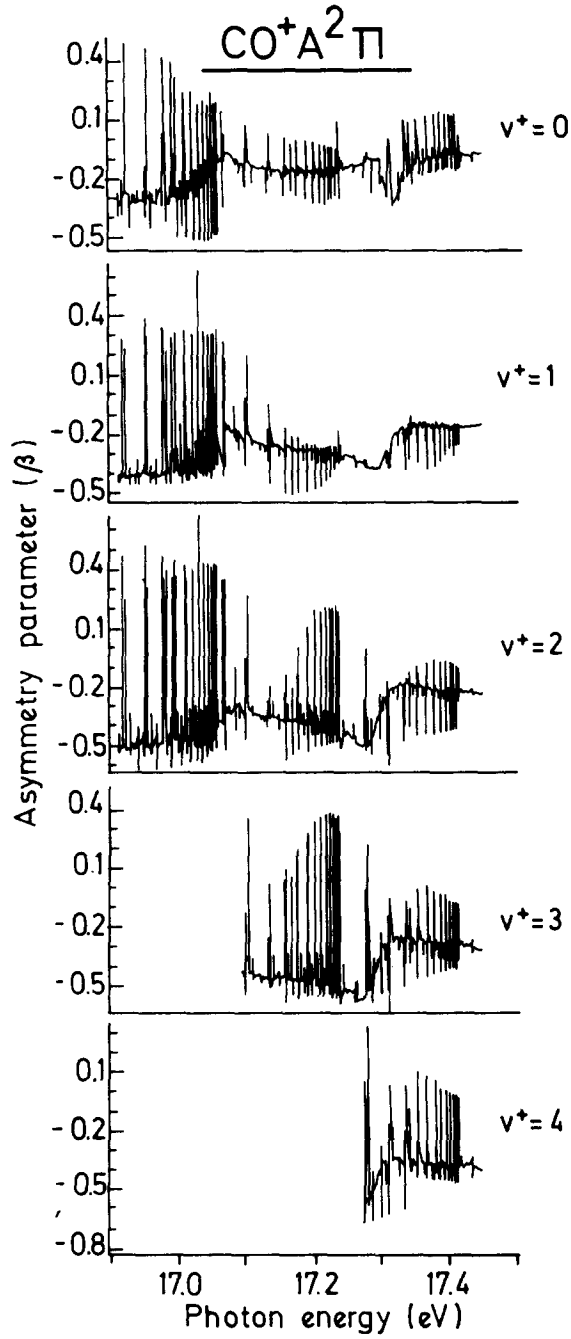

FIG. 7. Variation with photon energy of the $A\,^2\Pi$ vibrationally resolved asymmetry parameter β.

terms around a resonance. Let us take the $R_B 3'p'\pi\nu_R = 0$ resonance and the $X\nu^+ = 0$ continuum (Fig. 10). Calculated σ and $\sigma\beta$ have both a maximum at the resonance energy and roughly the same energy dependence around it. So to say, X, Y, and Z of Eq. (4) have values close to the values of A, B, and C of the integrated cross section $\sigma = (A\epsilon^2 + B\epsilon + C)/(1+\epsilon^2)$ (see Ref. 38). Looking in greater detail to the situation at resonance as compared to the situation around it, we see that the interference terms have a greater negative contribution at resonance then around it. It follows that at resonance X, Y, and Z are comparatively lower than A, B, and C thus giving a minimum in the β curve. The above described behavior appears also for the other resonances and the other continua associated with the X ionic state. To fit the experimental behavior, i.e., a maximum in β, X, Y, and Z should be larger than A, B, and C and their behavior at and around the resonance inverse to the one discussed above. It follows that the interference terms of X, Y, and Z are not calculated accurately enough to reproduce the experiment.

The case of the A ionic state is different as the calculated vibrationally resolved results (Fig. 9) show a broad maximum in β near 17.05 eV instead of a narrow minimum at 17.12 eV in the electronic calculation of β of LR (Fig. 3). The situation is different from the X continua where the electronic and vibrationally resolved results show the same mini-

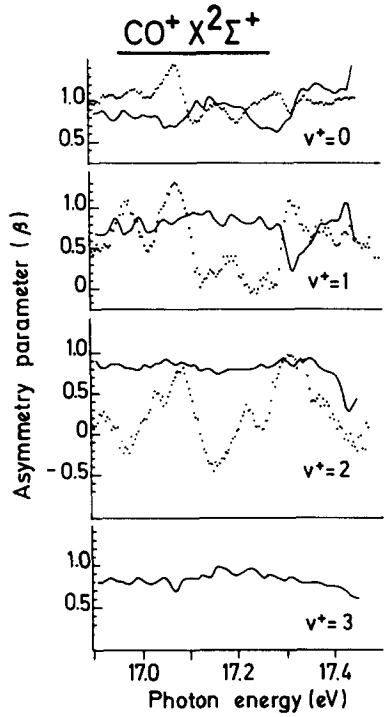

FIG. 8. Variation with photon energy of the $X\,^2\Sigma^+$ vibrationally resolved asymmetry parameter β. Solid line: theoretical results convoluted to a resolution of 0.017 eV (0.065 nm). Dotted line: experimental results of Hardis *et al.* (Ref. 25).

mum at resonance. Unfortunately no experimental results are available. From Fig. 10 we can infer that the coefficients of the second order energy polynomial [see Eq. (4)] describing the displayed resonances are very different in the case of $\sigma\beta$ and σ. The interference terms bring decidedly an important contribution to $\sigma\beta$, changing its energy dependence as compared to the angular integrated cross section σ.

This discussion leads us to the following question. Why is the agreement between theory an experiment better for the

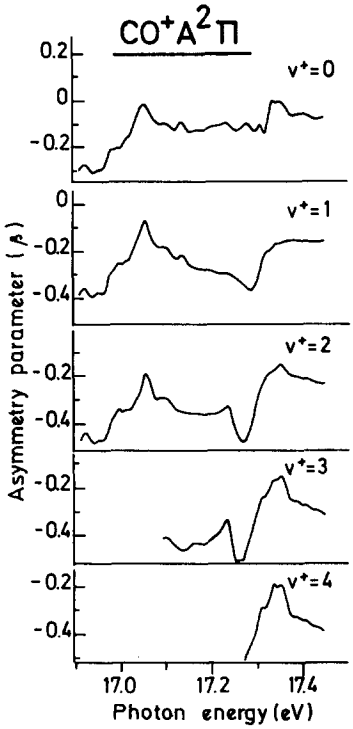

FIG. 9. Convoluted vibrationally resolved β parameter for the $A\,^2\Pi$ state. The width of the apparatus function is 0.017 eV (0.065 nm).

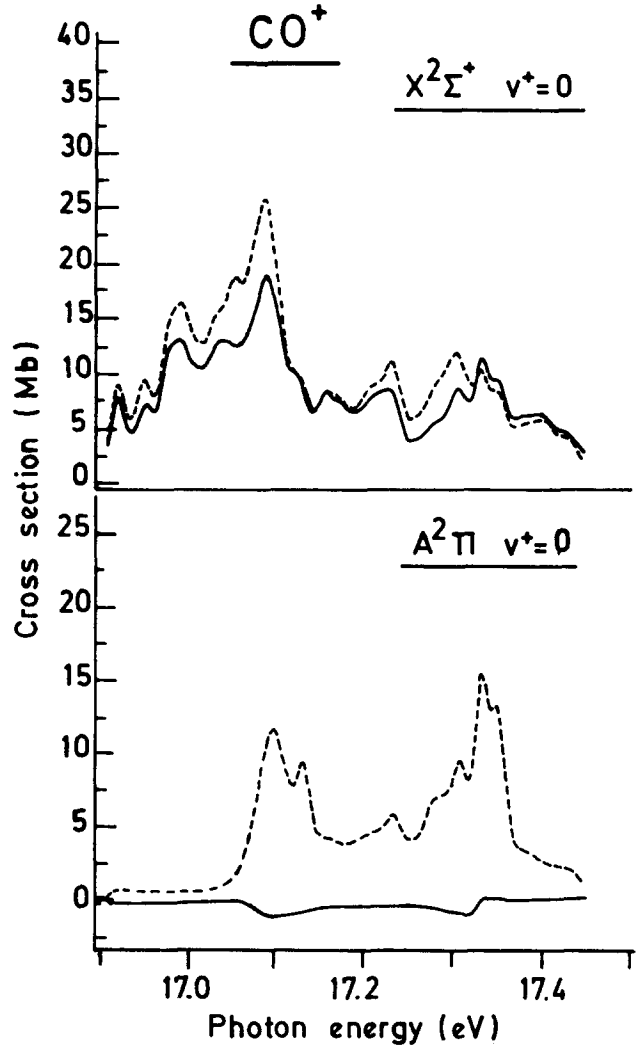

FIG. 10. Theoretical curves of σ (dashed line) and $\sigma\beta$ (solid line) for the $X\,^2\Sigma^+ v^+ = 0$ state and for the $A\,^2\Pi\ v^+ = 0$ state. These results are broadened to a resolution of 0.017 eV.

angular integrated cross sections σ than for the β curves? The weaknesses of our treatment can be summarized as follows. We use *ab initio* electronic quantities which are calculated in the one-configuration approximation. This is not sufficient for very accurate results. We also use the Condon approximation which neglects completely the pure vibrational autoionization: this does not allow the correct distribution of the intensity among the different channels. Finally, as was mentioned in Ref. 22, the presence of dissociation continua above 70 nm should also be taken into account in a complete treatment. As the β parameter results from a complicated balance of many interference terms, it is expected to be much more sensitive to these approximations than the integrated cross sections σ. At the present stage, it is unfortunately not possible to decide which approximation is most likely to break down.

V. CONCLUSIONS

The present approach is an attempt to perform a complete *ab initio* electronic and vibrational calculation which

takes into account all the photoionization molecular channels. Three electronic ionic cores with their respective vibrational levels have been considered. This calculation is therefore comparable with the two recent available experimental works on CO photoionization with vibrational resolution.[22,25] However, we have to point out that the electronic quantities have been calculated in the one configuration approximation. We have made use of Condon approximation, i.e., we have neglected the "pure" vibrational autoionization and dissociation.

The complicated resonant structures appearing between 17 and 17.5 eV (Figs. 1 and 2) can be systematized introducing the notions of complex[12,13] and composite resonances. Around 17.05 and 17.35 eV, the R'_A $(n+1)s + nd'\sigma, n'd'\delta$ and $n'd'\pi (n \geqslant 10)$ states converging to the $v^+ = 3$ and 5 thresholds, respectively, interact with the $R_B 3'p'\sigma$ and $3'p'\pi$ states; these R_A and R_B states interact with the $X\,^2\Sigma^+ v^+$ continua. Such a situation is usually referred to as a complex resonance. This means that, strictly speaking, the assignments given in LR in terms of R_B states only are oversimplified: the structures at 17.05 and 17.35 eV are to be assigned to complex resonances involving both the low-n R_B states and the high-n R_A states.

On the other hand, the resonant structure located around 17.2 eV results only from R_A states after a convolution procedure which takes into account the experimental resolution. Interaction with the R_B states is negligible. There are several molecular R_A series contributing to this unique structure and we have therefore named this resonance a composite resonance. This resonance has been first identified by Ogawa and Ogawa[24] as being the superposition of five members ($n = 9$, 10, and 11) of the $R_A v_R = 4$ series and of two members ($n = 7,8$) of the $R_A v_R = 5$ series. In fact, many Rydberg states with $n \geqslant 10$ are present in this region dominated by the same $'(n+1)s + nd'\sigma$, $n'd'\delta$ and $n'd'\pi$ series.

These resonances affect both the branching ratios between the different open channels and the asymmetry parameter β. Our results show that, for the $X\,^2\Sigma^+ v^+$ channels, the Condon approximation can be considered as satisfactory: these continua are essentially populated by electrostatic autoionization of the R_A and R_B series. The situation is completely different for the $A\ ^2\Pi\ v^+$ continua: the comparison between the experimental and theoretical results show that an interplay between electrostatic and pure vibrational Sec. IV, the disagreement between the experimental and theoretical differential cross sections (and β parameter) is greater owing to the difficulty in calculating accurate interference terms.

Experimentally, the appearance of such complex and composite resonances is hard to probe, even at the highest resolution one can presently obtain with synchrotron radiation. Such resonances are however very likely to be frequently encountered and are well worth a detailed study at the highest possible resolution: the use of VUV tunable lasers could lead to major progress in this field and to significant tests of the theoretical calculations.

Finally, we would like to stress that elaborate models such as the one presented in this paper can lead to new qualitative insight into the mechanisms of molecular photoionization, which could not be reached by oversimplified models.

ACKNOWLEDGMENTS

We are very grateful to Dr. Helene Lefebvre-Brion for her encouragements during this work and for many fruitful discussions. We acknowledge financial support by the F. N. R. S. (Belgium), the Belgian Government (Contrat d' Actions De Recherches Concertees), and the N. A. T.O. (Contract No. 096/82). B. L. is also indebted to the F. N. R. S. (Belgium) for the award of a research assistantship. We thank Mr. E. Massau for his assistance in the drawing of the figures.

[1] J. L. Dehmer, A. C. Parr, and S. H. Southworth, in *Handbook on Synchrotron Radiation*, edited by G. V. Marr (North-Holland, Amsterdam, 1987), Vol. II, p. 241.
[2] V. McKoy, T. A. Carlson, and R. R. Lucchese, J. Phys. Chem. **88**, 3188 (1984).
[3] I. Nenner and J. A. Beswick, in *Handbook on Synchrotron Radiation*, edited by G. V. Marr (North-Holland, Amsterdam, 1986), Vol. II, p. 355.
[4] M.-J. Hubin-Franskin, J. Delwiche, and P. M. Guyon, Z. Phys. D **5**, 203 (1987).
[5] F. Keller and H. Lefebvre-Brion, Z. Phys. D **4**, 15 (1986).
[6] G. Raşeev, B. Leyh, and H. Lefebvre-Brion, Z. Phys. D **2**, 319 (1986).
[7] H. Lefebvre-Brion and R. W. Field, *Perturbations in the Spectra of Diatomic Molecules1986* (Academic, Orlando, 1986).
[8] P. Morin, I. Nenner, M. Y. Adam, M.-J. Hubin-Franskin, J. Delwiche, H. Lefebvre-Brion, and A. Giusti-Suzor, Chem. Phys. Lett. **92**, 609 (1982).
[9] M.-J. Hubin-Franskin, J. Delwiche, P. Morin, M. Y. Adam, I. Nenner, and P. Roy, J. Chem. Phys. **81**, 4246 (1984).
[10] A. C. Parr, D. L. Ederer, J. B. West, D. M. P. Holland, and J. L. Dehmer, J. Chem. Phys. **76**, 4349 (1982).
[11] E. D. Poliakoff, M.-H. Ho, M. G. White, and G. E. Leroi, Chem. Phys. Lett. **130**, 91 (1986).
[12] A. Giusti-Suzor and H. Lefebvre-Brion, Phys. Rev. A **30**, 3057 (1984).
[13] A. Giusti-Suzor and H. Lefebvre-Brion, In *Photophysics and Photochemistry Above 6 eV*, edited by F. Lahmani (Elsevier, Amsterdam, 1985).
[14] A. Giusti-Suzor and H. Lefebvre-Brion, Chem. Phys. Lett. **76**, 132 (1980).
[15] A. Giusti-Suzor and Ch. Jungen, J. Chem. Phys. **80**, 986 (1984).
[16] M. Raoult, H. Le Rouzo, G. Raşeev, and H. Lefebvre-Brion, J. Phys. B **16**, 4601 (1983).
[17] B. Leyh and G. Raşeev, Phys. Rev. A **34**, 2920 (1986).
[18] G. Raşeev and H. Le Rouzo, *Abstracts of Contributed Papers-XIII. ICPEAC* (1983), p. 36; Ch. Greene, Phys. Rev. A **28**, 2209 (1983); H. Le Rouzo and G. Raşeev, *ibid.* **29**, 1214 (1984).
[19] G. Raşeev, J. Phys. B **18**, 423 (1985).
[20] A. L. Sobolewski and W. Domcke, J. Chem. Phys. **86**, 176 (1987).
[21] A. L. Sobolewski, J. Chem. Phys. **87**, 331 (1987).
[22] B. Leyh, J. Delwiche, M. -J. Hubin-Franskin, and I. Nenner, Chem. Phys. **115**, 243 (1987).
[23] R. E. Huffman, J. C. Larrabee, and Y. Tanaka, J. Chem. Phys. **40**, 2261 (1964).
[24] M. Ogawa and S. Ogawa, J. Mol. Spectrosc. **41**, 393 (1972).
[25] J. E. Hardis, T. A. Ferrett, S. H. Southworth, A. C. Parr, P. Roy, J. L. Dehmer, P. M. Dehmer, and W. A. Chupka, J. Chem. Phys. **89**, 812 (1988).
[26] K. P. Huber and G. Herzberg, *Molecular Spectra and Molecular Structure. Constants of Diatomic Molecules* (Van Nostrand Reinhold, New York, 1979), p. 166.
[27] J. C. Tully, R.S. Berry, and B. J. Dalton, Phys. Rev. **176**, 95 (1968).
[28] W. Thiel, Chem. Phys. Lett. **87**, 249 (1982).
[29] W. Thiel, Chem. Phys. **77**, 103 (1983).
[30] N. M. Kabachnik and I. P. Sazhina, J. Phys. B **9**, 1681 (1976).
[31] J. M. Delaval and G. Raşeev (unpublished results).
[32] R. S. Berry, J. Chem. Phys. **45**, 1228 (1966).

[33]K. Ito, A. Tabche-Fouhaile, H. Frohlich, P. M. Guyon, and I. Nenner, J. Chem. Phys. **82**, 1231 (1985).
[34]J. Berkowitz and W. A. Chupka, J. Chem. Phys. **51**, 2341 (1969).
[35]M. Raoult and Ch. Jungen, J. Chem. Phys. **74**, 3388 (1981).
[36]Y. Ono, S. H. Linn, H. F. Prest, C. Y. Ng, and E. Miescher, J. Chem. Phys. **73**, 4855 (1980).
[37]J. Berkowitz and J. P. Greene, J. Chem. Phys. **81**, 4328 (1984).
[38]D. L. Ederer, A. C. Parr, B. E. Cole, R. Stockbauer, J. L. Dehmer, J. B. West, and K. Codling, Proc. R. Soc. London Ser. A **378**, 423 (1981).
[39]U. Fano, Phys. Rev. **124**, 1866 (1961).